Limitations of curvature–induced rigidity: How a curved strip buckles under gravity

M. Taffetani[1], F. Box[1], A. Neveu[1] and D. Vella[1]

[1] *Mathematical Institute, University of Oxford, Woodstock Rd, Oxford, OX2 6GG, UK*

PACS 46.32.+x – Static buckling and instability
PACS 46.70.De – Beams, plates and shells
PACS 62.20.D- – Elasticity

Abstract – The preference of thin flat sheets to bend rather than stretch, combined with results from Geometry, mean that changes in a thin sheet's Gaussian curvature are prohibitively expensive. As a result, an imposed curvature in one principal direction inhibits bending in the other: so-called curvature-induced rigidity. Here, we study the buckling behaviour of a rectangular strip of finite thickness held horizontally in a gravitational field, but with a transverse curvature imposed at one end. The finite thickness of the sheet limits the efficacy of curvature-induced rigidity in two ways: (i) finite bending stiffness acts to 'uncurve' the sheet, even if this costs some stretching energy, and (ii) for sufficiently long strips, finite weight deforms the strip downwards, releasing some of its gravitational potential energy. We find the critical imposed curvature required to prevent buckling (or, equivalently, to rigidify the strip), determining the dependence on geometrical and constitutive parameters, as well as describing the buckled shape of the strip well beyond the threshold for buckling. In doing so, we quantify the intuitive understanding of curvature-induced rigidity that we gain from curving the crust of a slice of pizza to prevent it from drooping downwards as we eat.

Introduction. – From everyday experience, one knows that bending the crust of a slice of pizza prevents it from drooping under its weight. Insight into this intuitive solution to a meal-time conundrum comes from Gauss' *Theorema Egregium* [1–3], which states that changes in Gaussian curvature require an energetic cost associated with stretching. In the case of thin sheets, for which bending is energetically favourable over stretching, imposing curvature in the transverse direction induces a resistance to bending in the longitudinal direction since the sheet must then stretch in order to deform (see fig. 1).

This curvature–induced rigidity [4] is limited, however, by the finite thickness of the sheet. A naturally flat rectangular strip can be bent isometrically into a cylindrical shape, maintaining zero Gaussian curvature, only if suitable bending moments are prescribed along all four edges to counter the bending resistance of the strip. This resistance to bending means that, without any imposed edge-moments, a strip with finite thickness will try to 'uncurve', even at the expense of incurring some stretching energy. For large imposed curvature, Barois *et al.* [5] showed that the transverse curvature relaxes with distance from the end at which it is imposed, vanishing beyond a persistence length L_p that is determined by a balance between the curvature and stretching of the strip. This persistence length is given in scaling terms as

$$\frac{L_p}{W} \sim \frac{W}{(tR)^{1/2}} \tag{1}$$

where W and t are the width and thickness of the strip, respectively, while R is the imposed radius of curvature.

A second consequence of finite thickness is a non-zero weight: a strip held horizontally in a gravitational field also deforms longitudinally (*i.e.* in the direction orthogonal to the imposed transversal curvature) to release some of its gravitational potential energy. In this paper, we study how these two consequences of finite thickness combine to limit the efficacy of curvature-induced rigidity in a gravitational field. We anticipate that as the ratio of bending to gravitational energies decreases, the longitudinal curvature in the strip increases. It is therefore instructive to examine the total energy of the system as a function of the longitudinal curvature. A description of the relations between stability, curvatures and convexity

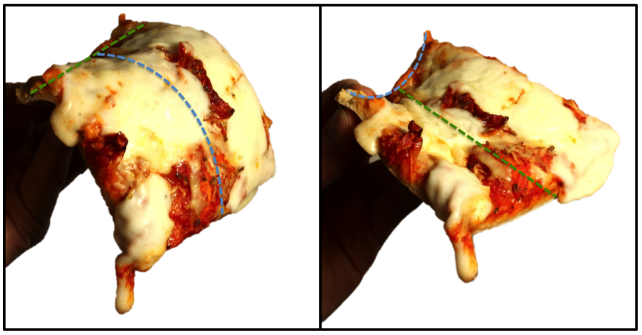

Fig. 1: A slice of pizza droops under its own weight (left). To prevent drooping, one instinctively bends the crust; this imposed curvature increases the effective rigidity of the slice, preventing drooping (right).

of this energy functional can be found in related studies [7, 8]. For a clamped transversely-flat cantilever beam [9], the total energy functional is a convex function of the imposed curvature: increases in the longitudinal curvature result in increased, yet continuous, bending of the beam. In contrast, a strip with uniform transverse curvature (*e.g.* a meter tape) can buckle suddenly [10], attaining large changes in shape as a result of small changes in longitudinal curvature. This potential for buckling is a direct consequence of the non-convexity of the total energy functional and corresponds physically to a change in sign of the moment required to impose a particular curvature. The situation we consider here has properties that lie between these two limiting cases, and the longitudinal curvature is induced by gravity acting on the strip of finite thickness. It is therefore natural to ask how a strip with imposed curvature at one end will respond to increasing gravitational loading or, equivalently, decreasing the imposed transverse curvature with fixed gravitational loading.

The geometry we consider is shown in fig. 2. There are four length scales in the problem: the geometrical properties of the strip (its length L, width W and thickness t), together with the radius of curvature that is imposed at one end, R. From the first three lengths, we construct two dimensionless parameters that characterize the geometry of the strip:

$$\lambda = \frac{L}{W}, \quad \tau = \frac{t}{L} \tag{2}$$

To rescale the imposed radius of curvature R we bear eq. (1) in mind and let

$$\kappa = \frac{W^2}{8Rt} \tag{3}$$

(the factor 8 is chosen so that $\kappa = \mathcal{Z}_0/t$ with $\mathcal{Z}_0 = (W/2)^2/(2R)$ the apparent thickness of the curved strip at the end where curvature is imposed). With this choice, eq. (1) becomes $L_p/W \sim \kappa^{1/2}$, and is found to hold provided that $\kappa \gtrsim 5$ [5].

To account for the role of gravity, we note that our strip has Young's modulus E and density ρ, and denote the gravitational acceleration by g. By balancing the bending modulus $B = Et^3W/12$ of a strip of rectangular cross section with the weight of the strip per unit length ρgtW, we extract an elasto-gravitational length $\ell_{eg} = (B/\rho gtW)^{1/3}$ [3, 11]. The relative strength of gravity is then given by the dimensionless parameter

$$G = \frac{L^3}{\ell_{eg}^3} = \frac{\rho gtW}{B} L^3 = \frac{12\rho g L^3}{Et^2}. \tag{4}$$

(Note that here we have taken the classical choice of the elasto-gravitational length, based on the heavy elastica equation [11]. However, we shall see that buckling is, in fact, controlled by the value of G/τ, rather than G alone.)

Given the plethora of dimensionless parameters in this problem, there are numerous ways in which limitations on the effectiveness of the curvature-induced stiffness could be quantified. In what follows, we shall assume that the strip's properties are given, so that the question reduces to determining the critical value of the curvature, $\kappa = \kappa^{(c)}(\lambda, \tau, G)$, at which the strip is effectively rigidified.

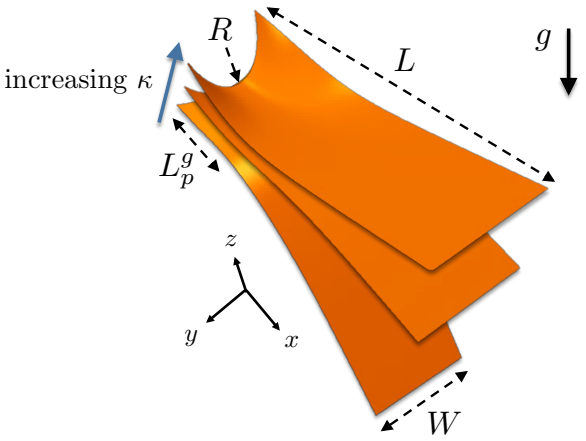

Fig. 2: Geometry of an elastic strip and its shape accommodation as a response to an increasing imposed curvature for a given gravitational load. For large enough imposed curvature, the strip is effectively rigidified against its own weight.

A simple view of the buckling threshold. – The state of the system is determined by a balance between a number of energetic terms. To better understand the balances involved we first recall the derivation [5] of the persistence length in the absence of gravity, L_p^0: this is obtained at a scaling level by optimizing the sum of the stretching energy $U_S \sim Et \cdot (\mathcal{Z}_0^2/L_p^2)^2 \cdot L_p w$ (which penalizes small L_p) and the bending energy $U_B \sim B \cdot (1/R)^2 \cdot wL_p$ (which penalizes large L_p). Minimizing the sum $U(G = 0) = U_B + U_S$ leads directly to the scaling (1), while a more detailed calculation [5] suggests that the prefactor in (1) is $\alpha_{\text{Barois}} = 2/\sqrt{35}$. In the presence of gravity, however, we expect that the gravitational potential energy of the strip will play an important role, possibly reducing

the length of the curved region, L_p^g, from its value in the absence of gravity. As a simple 'toy' model of the effect of gravity in this problem, we consider the gravitational potential energy of just the flat portion of the strip (beyond the part that is curved), *i.e.* $L_p^g < x < L$. Modelling this portion as an uncurved cantilever, the vertical deflection of the strip's end under gravity, $w_{\rm end} \sim \rho g t (L - L_p^g)^4/B$; the gravitational potential energy of this portion of the strip is thus $U_G \sim (\rho g t)^2 (L - L_p^g)^5/B$. Combining these energies, we have the total energy $U_{\rm tot}$, which may be written in dimensionless form as

$$\frac{U_{\rm tot}}{Et^5 w/L^3} = -\alpha_G \left(\frac{G}{\tau}\right)^2 (1-\tilde{L_p^g})^5 + \alpha_S \frac{\kappa^4}{(\tilde{L_p^g})^3} + \alpha_B \lambda^4 \kappa^2 \tilde{L_p^g} \tag{5}$$

where $\tilde{L_p^g} = L_p^g/L < 1$ is the proportion of the strip that remains curved. (We have explicitly introduced the constants of proportionality α_G, α_S and α_B to label the relevant terms as originating with the gravitational, stretching and bending energies, respectively.)

To understand the effect of gravity better, we assume that its effect is perturbative, that is that $L_p^g = L_p^0 + \delta L$ for some $\delta L/L_p^0 \ll 1$. Minimizing the energy in (5) we find that $L_p^0 = (3\alpha_S/\alpha_B)^{1/4} \kappa^{1/2} W$, in accord with the scaling of (1) and, further, that

$$L_p^g - L_p^0 \sim -\frac{G^2}{\tau^2} \frac{(1-L_p^0)^4 (L_p^0)^5}{\kappa^4} \tag{6}$$

As expected, this leading order expression shows that the effect of gravity is to reduce the portion of the strip that remains curved, decreasing L_p^g from its value in the absence of gravity. To see the effect of this decrease in L_p, note that the vertical deflection of the strip's end, $w_{\rm end} \sim -\rho g t (L - L_p^g)^4/B$, and hence

$$w_{\rm end} \sim -G(L - L_p^0)^4 \left[1 + \alpha \frac{G^2}{\tau^2 \lambda^8} \left(\frac{L - L_p^0}{L_p^0}\right)^3\right] \tag{7}$$

for some constant α. Hence, as the strength of the gravitational field increases, the deflection of the far end increases also, as should be expected. To highlight the effect of the gravity-induced lengthening of the flat portion (shortening of the curved region), we consider the rate at which $|w_{\rm end}(G)|$ increases as G increases: even for small G, increases in G increase $|w_{\rm end}|$ since the flat end is displaced. However, the shortening of the curved region enhances this effect, as can be seen by considering the rate of change of $w_{\rm end}(G)$, $w'_{\rm end}(G)$, relative to its value as $G \to 0$. We find that

$$\frac{w'_{\rm end}(G)}{w'_{\rm end}(0)} - 1 \sim \frac{G^2}{\tau^2 \lambda^8} \left(\frac{L - L_p^0}{L_p^0}\right)^3. \tag{8}$$

In particular, when $G = G_c$ with

$$\frac{G_c}{\tau \lambda^4} \sim \left(\frac{L - L_p^0}{L_p^0}\right)^{-3/2} \tag{9}$$

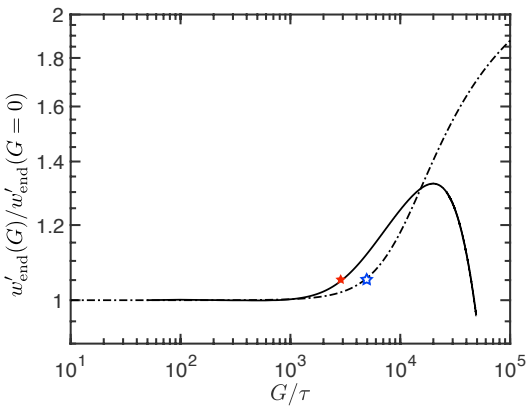

Fig. 3: The buckling transition is evidenced in the evolution of the height of the strip end, $w_{\rm end}$ as the strength of gravity changes. In particular, results from the toy model described here (dash-dotted curve) and Finite Element simulations (solid curve), described in the next section, show a marked increase beyond a critical value of G/τ. In both models, buckling is defined to be where this parameter reaches a critical threshold of 1.05, indicated by the stars. (Here $\kappa = 45$, $\lambda = 12$.)

we expect a large increase in the rate at which the deflection of the end of the strip increases with further increases in the strip weight G.

For this toy problem the energy, $U_{\rm tot}(\tilde{L_p^g})$, of (5) may be readily minimized numerically for various values of the parameters κ, λ and G/τ and chosen values of the coefficients α_G, α_S and α_B. Here we take $\alpha_S/\alpha_B = \alpha^4_{\rm Barois}/3$, to ensure we recover the result of Barois *et al.* as $G/\tau \to 0$ and $\alpha_G/\alpha_B = 1/5$ for convenience. The associated end displacement $w_{\rm end}(G)$ can also be calculated, at a scaling level, leading to plots for $w'_{\rm end}(G)$ such as that shown in the dashed curve of fig. 3. The results of such computations reveal a transition in $w'_{\rm end}(G)$ at a critical value of G that is consistent with the scaling in (9): the critical gravitational strength required to induce buckling increases as the length of the strip approaches (from above) the persistence length of the imposed curvature in the absence of gravity, L_p^0. Physically, this scaling suggests that buckling is brought about by gravity reducing the length of the curved region, L_p^g, to the point that the uncurved region becomes long enough to bend significantly under its own weight. To test the relevance of this simple-minded approach to the buckling transition of a strip under gravity, we now turn to a series of finite element simulations.

Numerical simulations. – A finite element model of the problem is implemented in the commercial software ABAQUS 6.14 (Dassault Systémes Simulia Corp., Johnstone, RI, USA). The strip is represented by a mesh of 4-node, doubly-curved shell elements (S4) and using a linearly elastic Hookean material. The analysis is carried out in two steps: in the first step, the transverse curvature is

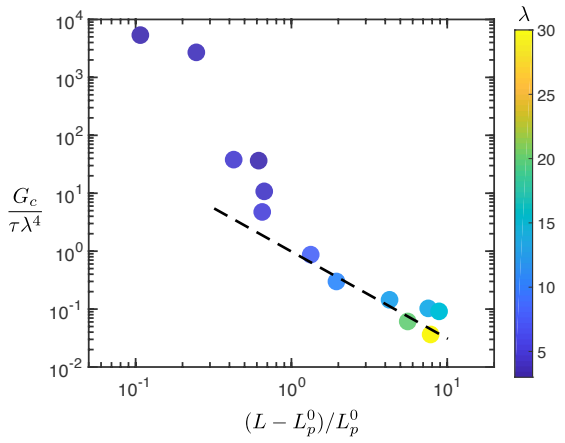

Fig. 4: The critical gravitational strength, G_c, plotted as a function of the ratio of the uncurved:curved portions of the strip in the absence of gravity, $(L-L_p^0)/L_p^0$. Numerical results are shown as points with colour coded according to the value of λ, as given in the colourbar. Plotted in this way, the prediction of the simplified model (9) becomes $y = x^{-3/2}$ (dashed line), and is recovered for sufficiently large values of $(L - L_p^0)/L_p^0$.

imposed at one extremity with no imposed gravity; the numerical problem is then to determine the variation of the curvature within the strip. In the second step, the magnitude of the gravitational load is increased via a sequence of static increments. It is worth noting that numerically it is easier to change G than to change the geometry of the strip (*i.e.* κ). No numerical stabilization is introduced.

Our simulations allow us to calculate $w'_{\rm end}(G)$, with the behaviour observed qualitatively similar to that observed in the toy model (see fig. 3). In these simulations, we definite the buckling event as the smallest G such that $w'_{\rm end}(G)/w'_{\rm end}(G=0) = 1.05$ (the stars in fig. 3). We then test the scaling suggested by eq. (9): in fig. 4, circles indicate the numerically calculated threshold, G_c, while the dashed line shows the scaling of (9). We see that the agreement is reasonable when $L \gg L_p^0$, *i.e.* cases for which the strip is mostly uncurved in the absence of gravity; however, the scaling prediction (9) breaks down when $L - L_p^0 \lesssim L_p^0$ — such strips are more rigid than would be expected from (9).

Further results for the behaviour in this critical region are shown in fig. 5. Note that in this study, we do not consider cases for which $L < L_p^0$ (the hatched area in fig. 5).

To understand how a finite strip thickness influences the critical curvature for buckling/rigidification, fig. 5 shows the qualitatively different behaviours that can be obtained for fixed values of λ, G/τ and $\nu = 0$ (here, $\lambda = 3$ and $G/\tau \approx 2.86 \times 10^3$). We obtain three types of behaviour as the imposed radius of curvature, κ, is varied: (A) For strong imposed curvature (large κ), the effect of gravity on the strip shape is negligible (variations in the transverse curvature result solely from the finite bending stiffness 'uncurving' the strip); (B) Close to the buckling threshold, the strip starts to feel the effect of gravity, deforming slightly downwards, and the imposed transverse curvature decays over a shorter distance than in (A); (C) For relatively small κ, the strip exhibits large-amplitude buckling with the far end of the strip orientated parallel to the direction of gravity. In this third case the strip comprises two distinct regions: an approximately horizontal region in which the transverse curvature decays with distance along the strip and a larger, approximately vertical, region in which the strip has lost any memory of the imposed transverse curvature, and is curved (in the longitudinal direction) solely by the effect of gravity. We revisit the behaviour in this highly deformed region later, but focus for now on further understanding the buckling transition.

Experiments. – The results of our numerical simulations suggest that the efficacy of curvature-induced rigidification is significantly enhanced for strips of comparable length to the persistence of curvature L_p^0, or λ close to $\kappa^{1/2}$. This feature that was not captured by our analysis of the toy energy functional (5). To test this conclusion further, we performed a set of experiments on strips of plastic (RS Pro Shim Kit, RS Components Ltd., Northants, UK). In particular, thickness and width values in the ranges $100 \le t \le 484\,\mu$m and $30 \le W \le 91$ mm were used, with the strip density $898\,\mathrm{kg\,m^{-3}} \le \rho \le 1464\,\mathrm{kg\,m^{-3}}$, Young's modulus 1.0 GPa $\le E \le$ 4.1 GPa and Poisson's ratio $\nu = 0.4$. (Young's modulus was determined via tensile tests using an Instron 3345 (Instron, Massachusetts, U.S.A)). Strips were clamped in a holder with radius of curvature $R = 4$ cm or $R = 5$ cm in such a way that the length of the strip L could be varied (G and λ were simultaneously varied whilst maintaining a constant κ). The strip was imaged using a DSLR camera (D7000, Nikon), with a spatial resolution of 0.02 mm/pixel, positioned orthogonal to the major axis of the strip. The profile of the strip was extracted from the images using detection techniques developed in MATLAB (Mathworks, Massachusetts, U.S.A). This enabled measurement of the variation in apparent thickness along the strip length and the deflection of the centreline of the strip shown in the inset to fig. 6. The critical length at which buckling occurred could then be determined from measurements of the displacement of the free end; the threshold was identified from abrupt changes in the displacement of the distal end that were observed as L is increased. These critical conditions $\kappa^{(c)}(\lambda, G/\tau)$ for buckling are represented by markers in fig. 6, to be compared with a further theoretical analysis.

Doubly curved model. – Returning to the buckling transition for $L - L_p^0 \lesssim L_p^0$, we now present a more detailed analysis of an analogue system. We begin by assuming that in this limit the primary effect of gravity is to impose a longitudinal curvature on the transversely curved ribbon(since there is very little uncurved ribbon remaining);

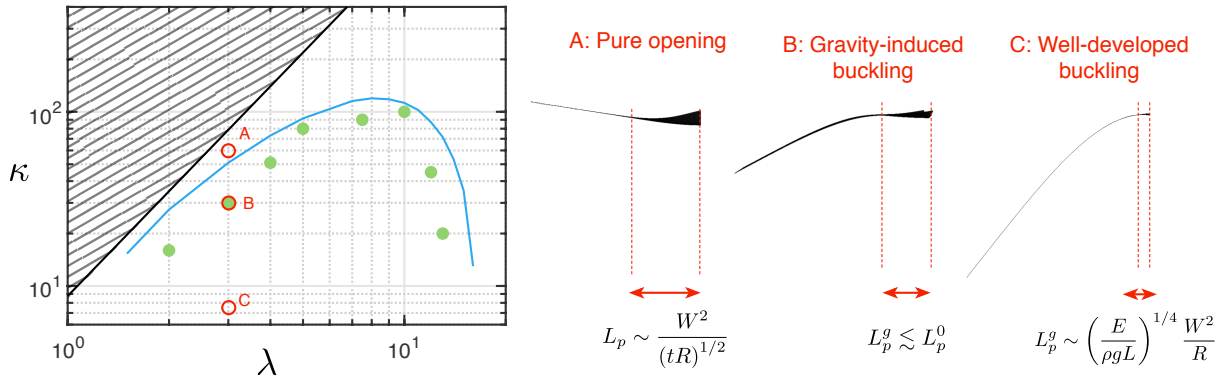

Fig. 5: Phase diagram for the imposed curvature at the onset of buckling as a function of the slenderness λ. The critical imposed curvatures $\kappa^{(c)}(\lambda, G/\tau)$ for $G/\tau = 2.8 \pm 0.1 \times 10^3$ obtained from FEM simulations are shown as green filled circles. The theoretical prediction from the doubly curved model is given by the continuous blue curve. To illustrate the behaviour as κ is varied with fixed λ and G/τ, the images on the right show the strip shapes obtained from finite element simulations; shapes with $\lambda = 3$, $G/\tau = 2.86 \times 10^3$ and three values of κ corresponding to the red open circles in the main plot.

we therefore consider the effect of an imposed curvature in the longitudinal (orthogonal) direction, K_L, (see fig. 7) and neglect any other effect of gravity. We shall find that there is a critical curvature K_L^c at which the ribbon buckles and then estimate the buckling threshold under gravity by equating this critical curvature to that induced by the self-weight of the strip.

For compactness, we describe here only the main ideas while the details are presented in the Supplementary Materials [6]. In the absence of gravity, we assume that the displacement field in the strip has the form $u = a_x(x)$, $v = 0$ and $w = a_z(x) + \mathcal{Z}$ where $\mathcal{Z} = c(x)y^2/2$ is the out-of-plane displacement relative to the displacement of the centreline, which is in turn determined from the functions $a_z(x)$ and $a_x(x)$ [5]. Rescaling curvatures by a factor $1/R$ the following dimensionless quantities can be introduced:

$$\gamma = cR; \quad \xi = \frac{x}{L}; \quad \eta = \frac{y}{W}; \quad \omega(\xi,\eta) = w(x,y)\frac{R}{W^2}; \\ \alpha_x(\xi) = a_x(x)\frac{R^2 L}{W^4}; \quad \alpha_z(\xi) = a_z(x)\frac{R}{W^2}. \tag{10}$$

We denote the dimensionless transverse curvature accommodated by the ribbon after the application of the dimensionless longitudinal curvature $\kappa_L = RK_L$ by $\gamma_{dc}(\xi)$; in general, the transverse curvature $\gamma_{dc}(\xi)$ is different from that of a strip opening purely under the presence of bending stiffness effects [5]. The relevant (dimensionless) energetic contributions are the stretching and bending energies in this regime, which we denote by $\mathcal{U}_S^{dc}$ and $\mathcal{U}_B^{dc}$, respectively, and may be written

$$\mathcal{U}_S^{dc} = 768\kappa^2 \int_0^{L_p/L} \int_{-\frac{1}{2}}^{\frac{1}{2}} \left(\bar{\epsilon}^{dc} - \lambda^{-2}\bar{\epsilon}\right)^2 \mathrm{d}\xi\mathrm{d}\eta \tag{11}$$

and

$$\mathcal{U}_B^{dc} = \int_0^{L_p/L} \int_{-\frac{1}{2}}^{\frac{1}{2}} \left[\left(\kappa_L + \lambda^{-2}\frac{\mathrm{d}^2\alpha_z}{\mathrm{d}\xi^2}\right)^2 + (\gamma_{dc} - \gamma)^2\right] \mathrm{d}\xi\mathrm{d}\eta \\ + \int_{L_p/L}^1 \int_{-\frac{1}{2}}^{\frac{1}{2}} \kappa_L^2 \mathrm{d}\xi\mathrm{d}\eta \tag{12}$$

where the stretching contribution is given by the dimensionless strain $\bar{\epsilon}^{dc} = -\eta^2\gamma_d c\kappa_L$ minus the longitudinal strain present before the application of κ_L and disregarding the higher order terms as in Barois *et al.* [5,6], as $\bar{\epsilon} = \mathrm{d}\alpha_x/\mathrm{d}\xi + (1/2)(\mathrm{d}\alpha_z/\mathrm{d}\xi)(\mathrm{d}\gamma/\mathrm{d}\xi)\eta^2 + (1/8)(\mathrm{d}\gamma/\mathrm{d}\xi)^2\eta^4$. Given this functional, we compute the transverse curvature $\gamma_{dc}(\xi)$ that minimizes the total energy $\mathcal{U}_{\mathrm{tot}}^{dc} = \left(\mathcal{U}_B^{dc} + \mathcal{U}_S^{dc}\right)$ and, in turn derive the (minimized) energy. This energy is non-convex as a function of the longitudinal curvature κ_L, so that buckling occurs [10, 15] at a critical longitudinal curvature $\kappa_L^{(c)}$ where $\kappa_L^{(c)}(G/\tau, \lambda) = \{\kappa_L : \partial^2\mathcal{U}_{\mathrm{tot}}^{dc}/\partial\kappa_L^2 = 0\}$.

Having determined the critical imposed longitudinal curvature $\kappa_L^{(c)}$ for a doubly-curved strip, we estimate the averaged longitudinal curvature in a ribbon with imposed transversal curvature under the influence of gravity. Since we assumed that buckling occurs while deformations remain small, we might imagine that both the transversal curvature and the persistence length do not change substantially compared to the case without gravity, *i.e.* $L_p^g \approx L_p$ (this approach is therefore not suitable to characterize strips with $L \leq L_p$). Within this approximation and using Mathematica (Wolfram Research Inc., Champaign, IL), it is possible to minimize the energy to derive analytical expressions for $\omega_g^{\mathcal{C}}$ and $\omega_g^{\mathcal{F}}$ so that the averaged longitudinal curvature (in the small strain approximation)

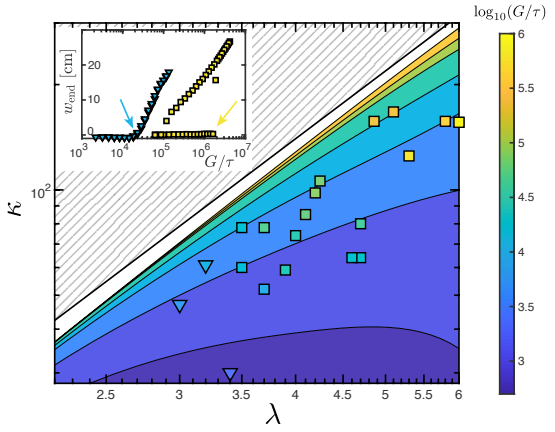

Fig. 6: Main figure: the critical curvature $\kappa^{(c)}$ at which buckling occurs for a given G/τ (with the value of G/τ represented by the colour coding indicated in the colourbar) as a function of the strip slenderness $\lambda = L/W$. The theoretical predictions from the doubly curved model (background colour) are compared with the experimental data (markers). (Perfect agreement would lead to experimental points being camouflaged against the background colour.) Square markers represent subcritical buckling under cyclical loading, while inverted triangles represent supercritical buckling. Inset: the displacement of the free end when buckling is subcritical (yellow squares) and when buckling is supercritical (blue inverted triangles); coloured arrows indicate the point at which buckling is determined to occur for the two cases shown.

in the ribbon is given by

$$\bar{\omega''} = \int_0^{L_p/L} \left(\frac{\mathrm{d}^2\omega_g^{\mathcal{C}}}{\mathrm{d}\xi^2}\right)\mathrm{d}\xi + \int_{L_p/L}^1 \left(\frac{\mathrm{d}^2\omega_g^{\mathcal{F}}}{\mathrm{d}\xi^2}\right)\mathrm{d}\xi = \left.\frac{\mathrm{d}\omega_g^{\mathcal{F}}}{\mathrm{d}\xi}\right|_{\xi=1} - \left.\frac{\mathrm{d}\omega_g^{\mathcal{C}}}{\mathrm{d}\xi}\right|_{\xi=0} \tag{13}$$

when continuity of the first derivative at $\xi = L_p/L$ is imposed. We take as the condition for the onset of buckling that the curvature of the strip induced by gravity, $\bar{\omega''}$, matches the critical imposed curvature at which the same strip will buckle, *i.e.*

$$\bar{\omega''} = \kappa_L^{(c)}. \tag{14}$$

The result of this theoretical analysis is shown by the continuous curve in fig. 5 and the background colourmap in fig. 6. The utility of this theoretical description is confirmed by comparisons between its predictions and the experimental measurements shown in fig. 6: here the critical curvature $\kappa^{(c)}$ at buckling is plotted as a function of λ for different G/τ. Both experiments and theory show that, for a given slenderness, λ, the curvature required to rigidify a strip against gravity increases with the ratio of gravitational to bending energy, G/τ. A further experimental observation is that that buckling is supercritical

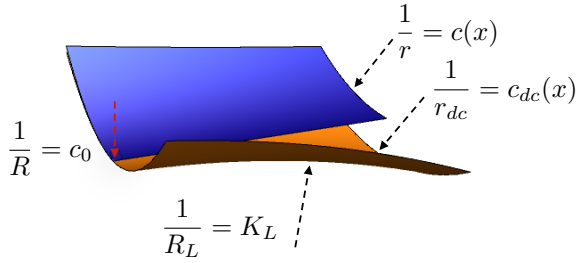

Fig. 7: The shape of a strip with a single imposed curvature (blue) is compared with the shape of a doubly-curved strip (orange). The transverse curvature is assumed positive and the longitudinal curvature negative, *i.e.* $-K_L$.

for small λ yet subcritical for large λ (discussed further in the Conclusion); even so, the predicted buckling threshold is in reasonable agreement with experiments in both cases. We note that, this analysis, and that provided earlier for strips long compared to L_p^0, give predictions for $\kappa^{(c)}(\lambda, G/\tau)$ when the persistence length L_p^g is not significantly changed from that in the absence of gravity; we now turn to consider how the persistence length of curvature, L_p^g, varies far beyond the buckling threshold.

Behaviour well beyond threshold. – Finally, we turn to the behaviour well beyond the buckling threshold; we assume again that the effect of the gravitational contribution in the domain $\mathcal{C}$ can be neglected and that $L_p^g \to 0$, so that may return to the earlier toy model. In this case, the gravitational energy of (5) must be revisited: now the displacement of the end is limited by the length of the strip, $w_{\rm end} \sim -(L - L_p^g)$, and hence $U_G \sim \rho g t W (L - L_p^g)^2$. We therefore replace the term $\alpha_G(1 - \tilde{L_p^g})^5 (G/\tau)^2$ of (5) with $\alpha_G(1-\tilde{L_p^g})^2(G/\tau)$. Moreover, we neglect the effect of the bending energy in (5) (since $G \gg 1$ and $L_p^g \ll 1$, we anticipate gravity and stretching dominate instead). We see from the modified (5) that minimizing the stretching energy requires the horizontal segment of the beam to be as long as possible (increasing L_p^g) while the release of gravitational potential energy pushes the system to decrease L_p^g. Minimizing the total energy allows us to determine the optimal persistence length of the imposed curvature:

$$\frac{L_p^g}{W} \sim \lambda \tau^{1/2} G^{-1/4} \kappa \tag{15}$$

where we require $L_p^g \ll L$. In terms of physical parameters, we find:

$$\frac{L_p^g}{W} \sim \left(\frac{E}{\rho g L}\right)^{1/4} \frac{W}{R}. \tag{16}$$

This prediction is evaluated in fig. 8 using experiments and FEM simulations: we observe a reasonable collapse, showing that our prediction is qualitatively correct.

Conclusion. – The weight of a rectangular ribbon of finite thickness, with an imposed transverse curvature at one end, acts to bend the strip against the imposed

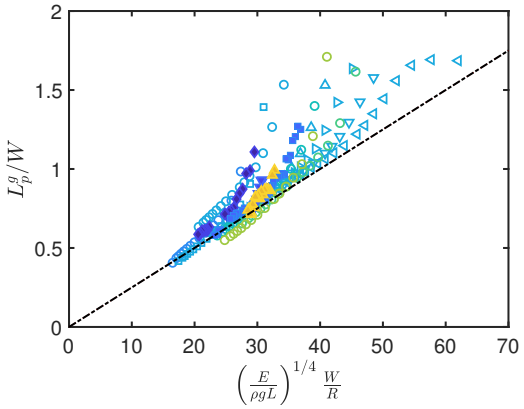

Fig. 8: The persistence length L_p^g well beyond the buckling threshold, measured for different geometrical and constitutive parameters (reported in the Supplementary Material [6]) in experiments (closed symbols) and finite element simulations (open symbols), collapse onto a single trend upon normalization: the slope of the black dash-dotted line is derived as a best fit of the FEM data to be 0.025.

curvature. Our analysis has shown that for strips that are long, $(L - L_p^0)/L_p^0 \gg 1$, the effect of gravity is to decrease the persistence length of the imposed curvature, enhancing the bending of the flat portion of the strip. In particular, (9) suggests in dimensional terms that the critical length of the flat portion of the strip

$$\frac{L - L_p^0}{\ell_{eg}} \sim \frac{\ell_{eg} t^{1/6}}{R^{1/2} W^{2/3}} \tag{17}$$

where $\ell_{eg} = (B/\rho g t)^{1/3}$ is the length beyond which a flat cantilever bends significantly [11].

As the strip length $L \searrow L_p^0$, a more detailed study of the energy of the system is required. We note that the structure of the energy functional we derived has similarities with the one discussed by Xuan and Biggins [16] for bead-on-string formation in stretched elastic cylinders subject to superficial tension. In our case, the *destabilizing* contribution is the increased applied longitudinal curvature that plays the same role that the applied stretch did in ref. [16]; this phenomenon is mainly controlled by the competition between the two orthogonal curvatures: the increasing longitudinal bending forces the strip to open transversely, partly relieving the longitudinal stretching. However, we have only considered strips of length $L < L_p^0$; to our knowledge, the problem of how buckling occurs for sufficiently weak curvatures that $L > L_p^0$ remains open.

Our experiments also suggest that the nature of the buckling changes depending on the imposed curvature. In the experiments, the buckling threshold is approached for a given G by varying L cyclically, and the tip deflection exhibits hysteresis for large imposed curvature. A formal understanding of this phenomenon is beyond the scope of this paper, but we note that the transition from subcritical (denoted by squares in fig. 6) to supercritical (denoted by inverted triangles in fig. 6) occurs for $\kappa \approx 60$, and the slenderness seems to have a minor effect. The subcritical nature of the buckling presents an additional danger for pizza-eaters, since, even within the stable, rigid regime, a small perturbation may cause a catastrophic reconfiguration of the strip from an almost horizontal configuration to the buckled shape, with the distal end of the slice orientated vertically, and with very messy consequences. Aside from the implications for eating habits, the work presented here provides a mechanical understanding of curvature-induced rigidity that might prove useful in applications such as the design of dielectric elastomer actuators with variable stiffness and tunable load capacity [17].

* * *

This research has received funding from the European Research Council under the European Union's Horizon 2020 Programme/ERC grant agreement no. 637334. We thank M. Gomez and O. Kodio for discussions about this work.

REFERENCES

[1] P. M. H. Wilson, *Curved spaces: From classical geometries to elementary differential geometry* (Cambridge University Press) 2008
[2] Numberphile, *The remarkable way we eat Pizza* (https://www.youtube.com/watch?v=gi-TBlh44gY) 2017
[3] Holmes D.P., *Curr. Opin. Coll. Interf. Sci.*, **40** (2019) 118–137
[4] Pini V., Ruz J.J., Kosaka P.M., Malvar O., Calleja M. and Tamayo J., *Sci. Rep.*, **6** (2016) 29627
[5] Barois T., Tadrist L., Quilliet C. and Forterre Y., *Phys. Rev. Lett.*, **113** (2014) 214301
[6] Taffetani M., Box F., Neveu A., and Vella D., *doi to be provided*, **xx** (xxxx) xxx-xxx
[7] Mansfield E.H., *Proc. R. Soc. Lond. A*, **334** (1973) 279-298
[8] Giomi L. and Mahadevan L., *Proc. R. Soc. Lond. A*, **468** (2012) 511-530
[9] Audoly B. and Pomeau Y., Oxford University Press (Editor), *Elasticity and Geometry* (Oxford) 2016
[10] Ponomarenko A., *Ecoulements critiques et plantes (PhD thesis)* (Universite Pierre et Marie Curie, Paris) 2012
[11] Wang C., *Int. J. Mech. Sci.*, **28** (1986) 549-559
[12] Ventsel E. and Krauthammer T., Marcel Dekker, Inc. (Editor), *Thin Plates and Shells - Theory, Analysis, and Applications* (New York) 2001
[13] Hohlfeld E. and Davidovitch B., *Phys. Rev. E*, **91** (2015) 012407
[14] Boltz H.-H. and Kierfeld J., *Phys. Rev. E*, **92** (2015) 033003
[15] James R.D., *J. Elast.*, **11** (1981) 239-269
[16] Xuan C. and Biggins J., *Phys. Rev. E*, **95** (2017) 053106
[17] Li W.-B., Zhang W.-M., Zou H.-X., Peng Z.-K. and Meng G., *Soft Robot.*, **00** (2019) doi: 10.1089/soro.2018.0046